Environmental control on eastern broadleaf forest species' leaf wax distributions and D/H ratios

Brett J. Tipple [a,*], Mark Pagani [b]

[a] *University of Utah, Department of Biology, 257 South 1400 East, Salt Lake City, UT 84112-0840, United States*
[b] *Yale University, Department of Geology and Geophysics, P.O. Box 208109, New Haven, CT 06520-8109, United States*

Abstract

Local climate and environment broadly affect the deuterium/hydrogen (D/H) ratios of plant materials, however the degree to which an individual plant's leaf waxes D/H ratios are affected by these parameters remains in question. Understanding these issues is particularly important in order to reconstruct past floral transitions and changes in the paleohydrologic cycle. For this study, we sampled five co-occurring tree species, *Acer rubrum*, *Platanus occidentalis*, *Juniperus virginiana*, *Pinus taeda*, and *Pinus strobus* and soils at forty sites along the East Coast of the US, from Florida to Maine. Hydrogen isotopic compositions of leaf wax *n*-alkanes, stem and surface waters were analyzed and compared against high-resolution temperature, precipitation, relative humidity, and vapor pressure deficit data to determine environmental controls on isotopic composition.

Our results demonstrate that each tree species produce a unique distribution of *n*-alkanes with distinct chain length pattern. Average *n*-alkane chain lengths recovered from soils, *A. rubrum*, and *J. virginiana* leaves show significant correlations with mean annual temperature. δD values of *A. rubrum* leaf *n*-alkanes were strongly correlated to modeled mean annual precipitation δD values and other climate parameters related to latitude (i.e. temperature, relative humidity, vapor pressure deficit), while the δD values of *J. virginiana* *n*-alkanes were not. Differences in correspondence may reflect the timing of leaf wax synthesis between the two species. Further, soil *n*-alkane D/H compositions were strongly correlated to modeled mean annual precipitation δD values, while the apparent hydrogen isotopic fractionation was not. These findings indicate that the isotope ratio of *n*-alkanes from soils in Eastern North American forests and similar ecosystems likely represents a time-averaged value that smooth out the environmental influence any one plant experiences.

© 2012 Elsevier Ltd. All rights reserved.

1. INTRODUCTION

The character and isotopic signature of higher plants and their molecular compounds are often applied to determine the terrestrial ecosystem's response to ancient climate change. However, our knowledge of modern higher-plant isotope chemistries and compound distributions in relation to climate variables is not well constrained (Sachse et al., 2012). Of particular significance is the application of stable hydrogen isotope values of leaf wax *n*-alkanes (δD$_{n\text{-alkane}}$) as proxies of "environmental water" (Sauer et al., 2001; Peters et al., 2005; Sessions, 2006; Eglinton and Eglinton,

2008). Hydrogen atoms of *n*-alkanes are covalently bonded to carbon atoms and have very slow exchange rates (10^4–10^8 years) in thermally immature sediments (Schimmelmann et al., 1999, 2006; Pedentchouk et al., 2006), making records of δD$_{n\text{-alkane}}$ excellent tools to interpret ancient hydrological characteristics. Nonetheless, fundamental questions regarding the relative importance of environmental versus biological controls of δD$_{n\text{-alkane}}$ signatures remain largely unexplored in modern natural ecosystems (Smith and Freeman, 2006; Feakins and Sessions, 2010) and controlled greenhouse experiments (Kahmen et al., 2011). Advancements are being made in this topic with the recent and widespread application of compound-specific hydrogen isotope analyses (CSIA) of terrestrial flora (Liu et al., 2006; Sachse et al., 2006, 2009; Hou et al., 2007a, 2008; Jia et al., 2008; Liu and Yang, 2008; Pedentchouk et al., 2008; McInerney et al., 2011; Zhang and Liu, 2011); however,

---

* Corresponding author.

E-mail addresses: brett.tipple@utah.edu (B.J. Tipple), mark.pagani@yale.edu (M. Pagani).

knowledge of environmental factors that control isotopic compositions of terrestrial plant material, including the importance of interspecies and intraspecies variation, is poor even though these records are increasingly used to interpret ancient environments (Sachse et al., 2012).

The hydrogen isotope ratio (D/H) of plant water and the resultant plant materials is closely associated with the hydrogen isotopic composition of environmental water, which is controlled by temperature, latitude, and regional weather patterns (Craig and Gordon, 1965; Rozanski et al., 1993; Gat, 1996; Dawson et al., 2002). Comparisons of $\delta D_{n\text{-alkane}}$ values with local precipitation and/or catchment water δD values suggest that at the basin, continental, and global scales, hydrogen isotope compositions of precipitation water the primary control on $\delta D_{n\text{-alkane}}$ (Sauer et al., 2001; Bi et al., 2005; Sessions, 2006; Hou et al., 2007a, 2008). Internal plant water D/H ratios can be further modified by soil rates of transpiration and/or evapotranspiration, which in turn are influenced by plant ecophysiology and environmental conditions (Dawson et al., 2002; Smith and Freeman, 2006; Hou et al., 2007a; Feakins and Sessions, 2010). Illustrating the difference between plant physiology and evaporative conditions, $\delta D_{n\text{-alkane}}$ values from deeply rooted plants in Californian chaparral and desert ecosystems show little evidence of soil evaporation in stem waters or n-alkanes (Feakins and Sessions, 2010), while shallow-rooted Great Plain grasses $\delta D_{n\text{-alkane}}$ values indicate that soil evaporation is an important influence (Smith and Freeman, 2006). In addition, leaf architecture specific to photosynthetic pathways (e.g. C_3 versus C_4), taxonomic classes (e.g. angiosperm versus gymnosperm), and growth forms (e.g. monocotyledons versus dicotyledons) are important controls on a plant's water-use characteristics, influencing the apparent isotopic fractionation between n-alkanes and source water ($\varepsilon_{n\text{-alkane}}$) with C_3 grasses $\varepsilon_{n\text{-alkane}}$ values averaging $\sim-170\permil$, C_4 grasses; $\sim-145\permil$, and C_3 trees and shrubs averaging $\sim-120\permil$ (Chikaraishi and Naraoka, 2003; Bi et al., 2005; Liu et al., 2006; Sachse et al., 2006; Smith and Freeman, 2006; Hou et al., 2007a; Pedentchouk et al., 2008). On regional scales, D/H compositions of plants derive primarily from the initial δD value of precipitation, the plant's functional type and any subsequent D-enrichment during evaporation in soils and/or evapotranspiration from leaves. Deconvolving the influence of these parameters is necessary to bolster the utility of $\delta D_{n\text{-alkane}}$ as a paleoclimate proxy (Sachse et al., 2012).

Ecophysiology studies of North American species using leaf wax δD values from natural ecosystems are weighted toward the arid western US west (Feakins and Sessions, 2010) and mid-west (Smith and Freeman, 2006; McInerney et al., 2011) with fewer studies on moist broad-leaf temperate Eastern forests (Hou et al., 2007a,b). Temperate forests of the Eastern United States have high relative humidity and precipitation amounts during the growing season, with multiple species that span the entire Eastern Seaboard, and thus provide the opportunity to assess the influence of latitudinal-varying environmental signals on specific species.

The molecular distribution of lipids is also influenced by environmental conditions and can act as a proxy for environmental temperature (Brassell et al., 1986; Schouten et al., 2002; Weijers et al., 2007). Distributions of n-alkanes from dust and marine sediment samples correspond to the temperature of n-alkane source region (Gagosian and Peltzer, 1986; Poynter et al., 1989; Simoneit et al., 1991). Recent studies show that the average n-alkane chain-length in aerosols correspond to precipitation and aridity, where regions of lower precipitation and higher aridity are characterized by higher-molecular weight n-alkanes (Schefuss et al., 2003).

Modern plants produce species-specific n-alkane distributions (Schefuss et al., 2003; Pedentchouk et al., 2008; Vogts et al., 2009) that vary with climatic parameters (i.e. temperature and precipitation) (Hughen et al., 2004), and C_4 grasses produce longer-chain n-alkanes compared to C_3 plants from similar environments (Rommerskirchen et al., 2006). Taxonomy (Rommerskirchen et al., 2006) and environmental conditions (Schefuss et al., 2003; Hughen et al., 2004; Sachse et al., 2009) are likely reasons driving molecular distributions. While the available data support links between n-alkane chain-length and environmental conditions, no study has tracked n-alkane chain-lengths of individual species across a climate gradient in order to determine contributing factors.

In this paper, we present stable hydrogen isotope compositions of higher-plant n-alkanes from specific C_3 angiosperm and gymnosperm tree species along a climate gradient in order to better understand environmental factors responsible for the hydrogen isotopic compositions of terrestrial plant materials. The chosen climate gradient allows us to assess environmental factors, such as precipitation and temperature, while limiting humidity and elevation effects. Here, we address if and how $\delta D_{n\text{-alkane}}$ values are influenced by temperature, precipitation, and/or relative humidity, as well as isotopic differences between angiosperm and gymnosperms. Finally, we attempt to understand how leaf wax lipid distributions are related to local climate.

2. MATERIALS AND METHODS

2.1. Sample localities and materials collected

Materials were collected twice during the growing season of year 2006 (July and August) from 40 sites along the East Coast of the United States (Fig. 1). The eastern coast of the US is a humid temperate domain under the Koppen-Trewartha ecoregion scheme (Bailey, 2002). Annual precipitation ranges from 1800 mm on the Florida Panhandle to $\sim$750 mm in Maine (McNab and Avers, 1994). Mean annual and seasonal temperatures and moisture delivery decrease towards the north, while relative humidity is rather invariant over the entire eastern United States with an average value of $70 \pm 2\%$ (1σ). Sample elevations range between 0 and 685 m above sea level and are characteristic of piedmont and coastal plain regions (McNab and Avers, 1994).

The transect covers a $>$100 mm summer precipitation range and a 13 °C mean annual temperature gradient with little variation in annual or seasonal relative humidity. Several ecoregion divisions are represented including warm

continental (high humidity, warm summers, continental climate), hot continental (high humidity, hot summers, continental climate), and subtropical (humid subtropical climate, no dry season) (Bailey, 2002). Two angiosperm (red maple, *Acer rubrum* L.; sycamore, *Platanus occidentalis* L.) and three gymnosperm species (redcedar *Juniperus virginiana* L.; loblolly pine, *Pinus taeda* L.; white pine, *Pinus strobus* L.) were selected as they are common species and co-occur together along the transect (Fig. 1).

To limit anthropogenic disturbance and potential contamination, all samples were collected from regional, state, and national wild lands. Individual trees were marked with GPS coordinates. Tree height, canopy cover, aspect, slope, distance to standing or moving water were noted for each individual tree. To limit canopy isotope effects, all samples were collected from open forest canopy coverage of less than 50% coverage. Three to six individual sun leaves (to control for irradiance) were harvested from each specimen between 1.8 and 2.4 m above the ground (to control for hydraulic conductance) and stored in adhesive-free envelopes. Leaves were only handled by the petiole and/or stem to limit contamination and wax abrasion. Leaves were oven dried overnight at 50 °C.

Stems 10–20 cm in diameter and 40–50 cm in length were clipped as near to the trunk as possible, immediately placed in thick-walled glass culture tube (Pyrex 25 × 150 mm, rimless) and capped with a double seal serum stoppers to limit water loss. Stems were frozen until stem water was extracted. To establish a baseline for comparison between stem waters and leaf waxes, surface waters were collected at most sites from nearby rivers and streams. Surface water were in 4 ml vials, capped, sealed with Parafilm®, and transported in a cooler. Surface waters were refrigerated prior to analysis.

In addition to plant materials, ∼100 g of the soil A-horizon (down to 15 cm) was collected at most localities by removing the duff with a hand trowel. Soil material was stored in a sterile, low hydrocarbon bleed Whirl Pak brand sample bags. Soils were dried for 24 h using a Labconco freeze drier and frozen prior to lipid extraction.

2.2. Lipid extraction

Leaf wax lipids were extracted from whole leaves and soils with 2:1 dichloromethane (DCM)/methanol by ultra-sonication (30 min × 2). Total lipid extracts were concentrated under a stream of purified nitrogen using a Zymark Turbovap II evaporator. Hydrocarbons were separated by column chromatography using 1 g deactivated silica gel and hexane. If needed, *n*-alkanes were separated from branched alkanes and alkenes/alkynes using urea adduction and silver nitrate treatment, respectively (Wakeham and Pease, 1992).

Compound abundances were determined using a Thermo Trace 2000 gas chromatograph (GC) fitted with a programmable-temperature vaporization injector and flame ionization detector (FID). A fused silica, DB-1 phase column (60 m × 0.25 mm I.D., 0.25 μm film thickness) was used with helium as the carrier at a flow of 2 ml/min. GC oven temperature program utilized was 60–320 °C at 15 °C/min with an isothermal for 30 min. *n*-Alkanes were

identified and quantified through comparison of elution times with *n*-alkane references at known concentrations.

2.3. Compound-specific isotope analysis

Isotope analyses were performed using a Thermo Trace 2000 GC coupled to a Finnigan MAT 253 isotope ratio mass spectrometer interfaced with a High Temperature Conversion system. GC column, carrier flow, and ramp conditions were identical to above. The H_3^+ factor was determined daily prior to standard calibration and sample analysis.

Isotopic compositions are calculated following:

$$\delta = \left[\left(\frac{R_{samp}}{R_{std}} \right) - 1 \right] \tag{1}$$

where R represents the D/H abundance ratio, and R_{samp} and R_{std} represent the sample and standard, respectively. Delta values are reported in permil notation, which implies a factor of 1000 (Coplen, 2011) and are expressed relative to Vienna Standard Mean Ocean Water (VSMOW). Individual *n*-alkane isotope ratios were calibrated using *n*-alkane standard reference materials (Arndt Schimmelmann's "Mix A") analyzed daily at several concentrations. In addition, 5α-androstane of known isotopic composition was co-injected to confirm standard corrections were appropriate. Analytical precision for *n*-alkanes isotope determinations was ±3‰ for δD analysis.

2.4. Stem water extraction

Stems were warmed to room temperature prior to stem water extraction. Sealed tube, stem, and serum stopper were weighed and placed in liquid nitrogen for 5 min to freeze water vapor. Serum stopper was then removed and the tube containing the stem was attached to a water extraction manifold coupled to a vacuum line system following West et al. (2006). Once vacuum was reached, U-shaped extraction chambers were closed and liquid nitrogen was removed from stem-side tube and a placed on a water collection vessel. Stem-containing tubes were allowed to warm to room temperature and then submerged in a hot oil bath (100 °C). Stem water collection was maintained for 1 h. A hot-air gun was used to remove any condensation trapped between the hot and cold arms of the extraction chamber. After 1 h, or when no condensation remained, vacuum was broken and the water collection vessel was capped with Parafilm, allowed to melt in a refrigerator and then immediately transferred to a pre-weighed 4 ml vial. Water weight was determined and vial was stored in the refrigerator prior to isotope analysis. After extraction, serum stopper was replaced on stem-containing tube and the stem, tube, and serum stopper were reweighed to determine weight of water removed. To determine if water was quantitatively extracted, stems were dried in an 80 °C oven for one week and then reweighed.

2.5. Water δD and δ^{18}O analysis

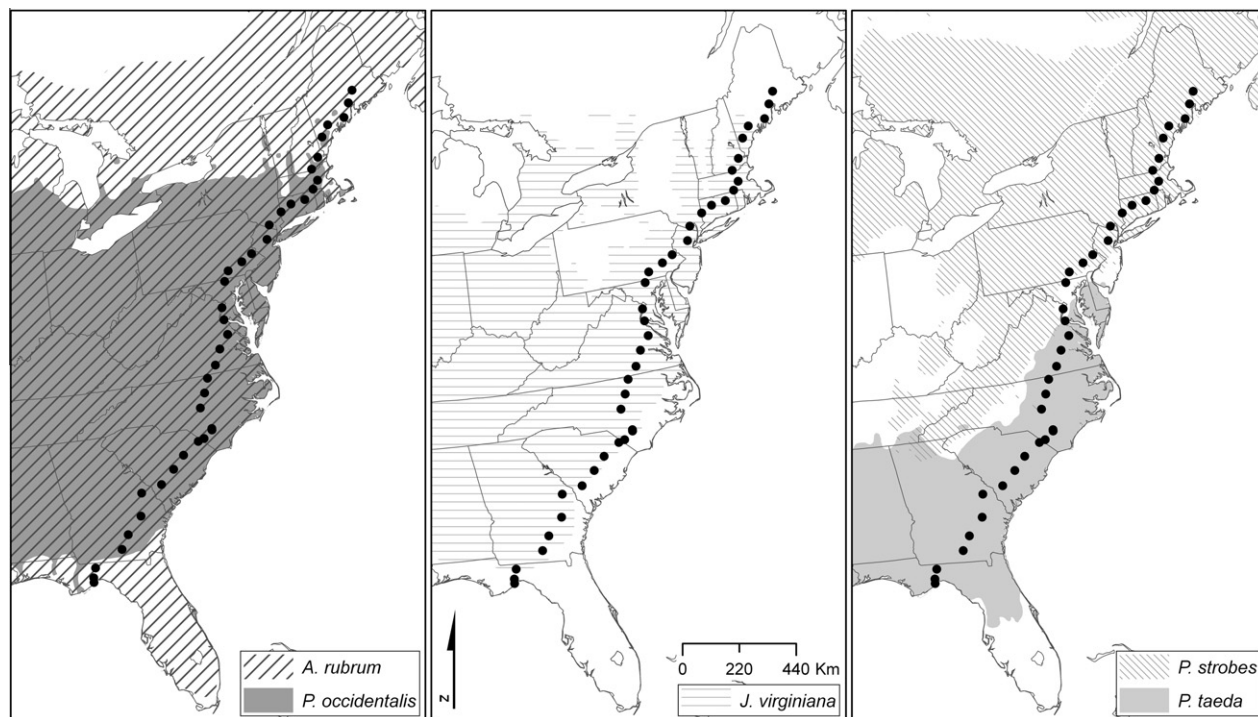Stem and surface water D/H compositions were analyzed using a ThermoFinnigan H-device interfaced to a

Fig. 1. Sample localities and distributions of sampled trees. Tree distributions produced from United States Geologic Survey's Digital Representations of Tree Species Range Maps.

ThermoFinnigan MAT 253 isotope ratio mass spectrometer. The liquid water (0.1 μl) was injected onto an 850 °C chromium granule column to produce Cr_2O_3 and H_2 gas. δD values are expressed relative to VSMOW and corrected to in-house water references (normalized to international standards) analyzed during sequence. The H_3^+ factor was determined daily prior to sample analysis. Analytical precision for water δD was $\pm 2\permil$ (1σ).

For $\delta^{18}O$ analysis, a 500 μl sub-sample was taken from each stem water and surface water sample and equilibrated for 24 h with 0.3% CO_2 with a known isotopic composition in He at approximately 26 °C. The $\delta^{18}O$ of the equilibrated CO_2 gas was analyzed using a GasBench II coupled to a ThermoFinnigan Delta^{plus}XP. Water $\delta^{18}O$ values are expressed relative to VSMOW. In-house reference materials were included with each sequence to allow for the empirical calculation of the isotopic equilibrium offset between water and CO_2. Analytical precision for water $\delta^{18}O$ was $\pm 0.2\permil$ (1σ).

2.6. Climate variables and geographical information systems

Site latitude, longitude, and elevation information were imported to geographical information software (ArcGIS 9.2) as a point shape (vector) file. The site vector layer was intersected with raster layers of the PRISM (Parameter-elevation Regressions on Independent Slopes Model) continuous, gridded climate data produced by the Oregon Climate Service (from http://www.ocs.orst.edu/prism/). PRISM is an analytical model of gridded estimates of monthly and annual precipitation and temperature measurements (as well as other climatic parameters). PRISM point measurements of temperature, precipitation, and dew point originated from some or all of the following sources: (1) National Weather Service (NWS) Cooperative stations, (2) Natural Resources Conservation Service (NRCS) SNOTEL, (3) United States Forest Service (USFS) and Bureau of Land Management (BLM) RAWS Stations, (4) Bureau of Reclemation (AGRIMET) stations, (5) California Data Exchange Center (CDEC) stations, (6) Storage guages, (7) NRCS Snowcourse stations, (8) Other State and local station networks, (9) Estimated station data, (10) Upper air stations, and (11) NWS/Federal Aviation Administration (FAA) Automated surface observation stations (ASOS). The PRISM climate datasets provide high spatial resolution (0.042° grid cells) for all years and months necessary for our analysis. The site vector layer was intersected with the PRISM mean annual temperature (MAT) and July mean precipitation (PPT). The PRISM mean July dew point temperature and mean July temperature were used to calculate mean July relative humidity (RH) following:

$$RH = \frac{e^{\left(\frac{17.269 \times T_d}{273.3 + T_d}\right)}}{e^{\left(\frac{17.269 \times T_{mean}}{273.3 + T_{mean}}\right)}} \times 100\%, \tag{2}$$

where T_d is the mean July dew point temperature and T_{mean} is the mean July temperature.

Monthly vapor pressure deficit (VPD) was calculated for each site. The saturation vapor pressure (e_s) was computed using the Tetens formula (Buck, 1981) following:

$$e_s = ae^{\frac{bT}{T+c}} \tag{3}$$

where T is the average monthly temperature (°C) and the constants a, b, and c are 0.611 kPa, 17.502, and 240.97 °C. The average monthly air vapor pressure (e_a) was determined by:

$$e_a = e_s \times \left(\frac{RH}{100\%}\right) \qquad (4)$$

where e_s and RH were determined from Eqs. (2) and (3). The vapor pressure deficit (VPD) is defined by:

$$VPD = e_s - e_a \qquad (5)$$

2.7. Statistical analysis

All statistical analyses were performed using JMP 9 (SAS, Cary, NC) with an α set at 1% for all analyses. Mean annual temperature, July relative humidity, July vapor pressure deficit, July precipitation, and mean annual precipitation δD value were extracted from the PRISM climate datasets and waterisotopes.org across the 40 sites. The relationship between climate data, average chain length, and $\delta D_{n\text{-alkane}}$ were analyzed using simple linear regressions. Principal component analysis (PCA) was used to identify patterns in the original data set, combine co-variables, and to facilitate the extraction of accumulated variables not directly measured. PCA provides an interpretable overview of the main information in a multidimensional data table. Here, PCA combines the initial variables onto a smaller number of components from which isotope values can be compared. An acceptable principal component solution

$$CPI = \frac{(A_{23} + A_{25} + A_{27} + A_{29} + A_{31} + A_{33}) + (A_{25} + A_{27} + A_{29} + A_{31} + A_{33} + A_{35})}{(2A_{24} + A_{26} + A_{28} + A_{30} + A_{32} + A_{34})}, \qquad (6)$$

was determined based on Cattell's Scree Test (Norman and Streiner, 2000) and component loadings.

3. RESULTS

3.1. Measured and modeled surface waters δD and $\delta^{18}O$ values

The δD values of streams and rivers (i.e. surface waters; δD_{SW}) express a 51‰ range along the East Coast (Table S1). δD_{SW} values are strongly correlated to latitude ($r = 0.99$, $p < 0.0001$; Fig. 2a). Surface water oxygen and hydrogen isotope ratios are positively correlated ($r = 0.96$, $p < 0.0001$) with a relationship of $\delta D_{SW} = 7.5\delta^{18}O_{SW} + 3.6$

(Fig. S1). These regional data are consistent with local surface water lines from Eastern Seaboard locations (Kendall and Coplen, 2001) and suggest the influence of kinetic effects associated with evaporation (Dansgaard, 1964). δD_{SW} values are strongly correlated to the hydrogen isotope compositions of modeled growing season (δD_{GSP}, $r = 0.94$, $p < 0.0001$) and modeled mean annual precipitation (δD_{MAP}, $r = 0.94$, $p < 0.0001$) (Fig. 3a). Slopes between δD_{SW} and δD_{GSP} and between δD_{SW} and δD_{MAP} are 0.60 and 0.93, respectively. Surface water δD values are 12‰ more D-enriched compared to modeled mean annual precipitation δD values. These data suggest East Coast surface water is weighted towards D-enriched summer precipitation or subject to evaporation.

3.2. Stem water δD values

Extractions were found to recover 99.8% of xylem water. The hydrogen isotope ratio of xylem water (δD_{XW}) from *A. rubrum* and *J. virginiana* stems ($n = 62$) demonstrated an overall variation of 47‰ (Table S1). δD_{XW} values are strongly related to latitude ($r = 0.96$, $p < 0.0001$; Fig. 2b) and hydrogen isotope compositions of surface water (δD_{SW}, $r = 0.87$, $p < 0.0001$), modeled growing-season (δD_{GSP}, $r = 0.79$, $p < 0.0001$) and mean annual precipitation (δD_{MAP}, $r = 0.81$, $p < 0.0001$). The relationship between δD_{XW} versus δD_{MAP} is nearly 1:1, suggesting ground water is equivalent to mean annual precipitation in this case (Fig. 3b). Furthermore, these results indicate that stem water δD values can be used interchangeable

with, and in place of, modeled δD_{MAP} values in these temperate broad-leaf forests.

3.3. Leaf wax compound distributions

We found no systematic variation of *n*-alkanes abundance with species or site location. Carbon preference indices (CPI) were calculated following Marzi et al. (1993):where "A" represents the area of the individual *n*-alkane peak from the chromatograph trace. Individual leaf and soil CPI values are shown in Table S2.

A. rubrum and *P. occidentalis* have an average CPI of 33.3 and 23.6, respectively. *J. virginiana*, *P. strobus* and *P. taeda* average 17.8, 6.8, and 9.6, respectively. Strong odd-

$$ACL = \frac{(A_{23}(23) + (A_{25}(25) + (A_{31}(27) + (A_{29}(29) + (A_{31}(31) + (A_{33}(33) + (A_{35}(35))}{(A_{23} + A_{25} + A_{27} + A_{29} + A_{31} + A_{33} + A_{35})}, \qquad (7)$$
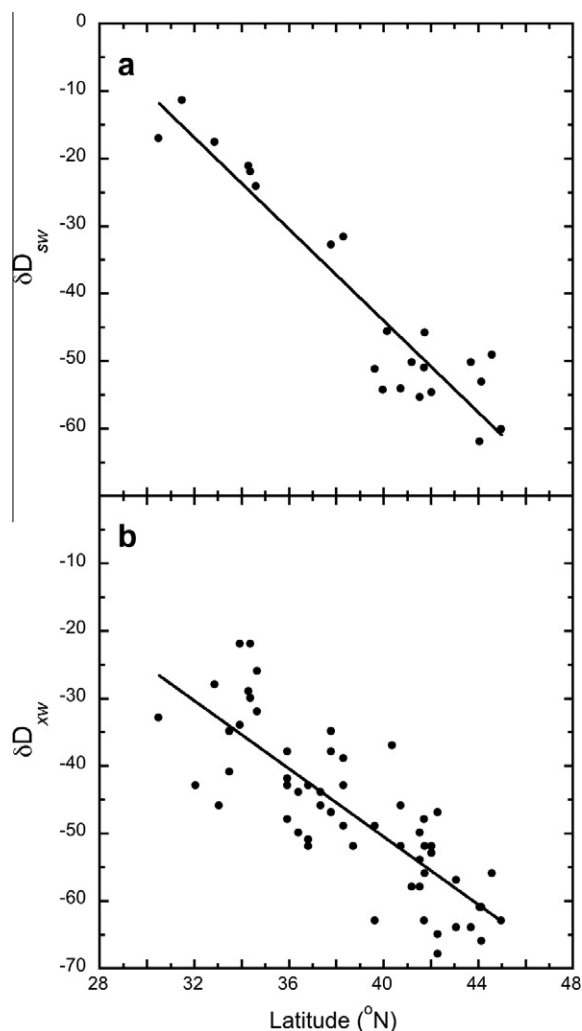
Fig. 2. Hydrogen isotope values of surface waters and stem waters versus latitude. (a) Hydrogen isotope values of surface waters and latitude are correlated ($r = 0.96$, $p < 0.0001$) with a regression line of $\delta D_{SFW} = -3.4 * Latitude + 92$. (b) Hydrogen isotope values of stem waters and latitude were correlated ($r = 0.96$, $p < 0.0001$) with a regression line of $\delta D_{XW} = -2.5 * Latitude + 50$.
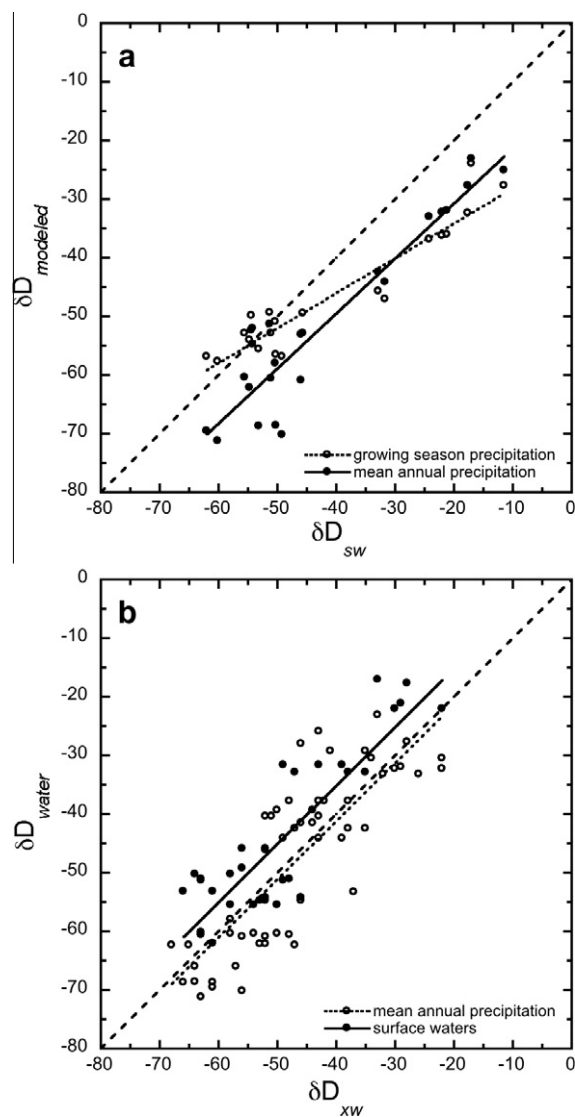

Fig. 3. (a) Hydrogen isotope values of mean annual and growing season precipitation versus surface water. Hydrogen isotope values of surface waters and mean annual and growing season precipitation were correlated (δD_{MAP}, $r = 0.94$, $p < 0.0001$ and δD_{GSP}, $r = 0.94$, $p < 0.0001$, respectively) with regression lines of $\delta D_{MAP} = 0.94 * \delta^2 H_{SFW} - 12$ and $\delta D_{GS} = 0.60 * \delta D_{SFW} - 22$. Dotted line represents 1:1 correspondence. (b) Hydrogen isotope values of mean annual precipitation and surface waters versus stem water. Hydrogen isotope values of stem water and mean annual and surface waters were correlated ($r = 0.87$, $p < 0.0001$ and 0.82, $p < 0.0001$, respectively) with regression lines of $\delta D_{SFW} = 0.99 - * \delta D_{XW} + 5$ and $\delta D_{MAP} = 0.99 * \delta D_{XW} - 1$. Dotted line represents 1:1 correspondence.

over-even predominance in modern leaf wax extractable *n*-alkanes is consistent with previous observations (Eglinton and Hamilton, 1967; Lockheart et al., 1997; Piasentier et al., 2000). Soil CPI values average 12.4, and range from 4.6 to 22.9.

A. rubrum was found to produce $n\text{-}C_{27}\text{-}C_{33}$ with $n\text{-}C_{31}$ as the most abundant *n*-alkane, while *P. occidentalis* produced $n\text{-}C_{25}\text{-}C_{33}$ with C_{25} and C_{27} as the most abundant alkanes (Fig. 4). *J. virginiana* produced *n*-alkanes with 31–35 carbon atoms with $n\text{-}C_{33}$ as the predominant *n*-alkane. *P. taeda* and *P. strobus* contained $n\text{-}C_{21}\text{-}C_{31}$ and $n\text{-}C_{23}\text{-}C_{31}$, respectively (Fig. 4).

We compiled peak areas of high molecular weight *n*-alkanes in order to quantify variations in distributions of *n*-alkanes. To relate changes in average chain length (ACL) we used the following:where "*A*" corresponds to the area of the individual *n*-alkane peak from the chromatograph

trace. Individual leaf and soil ACL values are shown in Table S2. We found that molecular distributions for individual species vary slightly (<10% change) across the entire transect. Soil ACL range from 28.8 to 30.5 and average 29.8, while *J. virginiana* ACL range from 33.0 to 33.7 and average 33.3 (Fig. S2). The angiosperms, *A. rubrum* and *P. occidentalis*, range from 27.4 to 30.6 and 28.0 to 32.3 and average 29.9 and 29.2, respectively. The pines, *P. taeda*

and *P. strobus*, range from 24.0 to 26.5 and 27.1 to 28.1 and average 24.9 and 27.8, respectively (Fig. S2).

Our results show that ACL is inversely related to latitude, with longer-chain lengths produced at lower latitude. Soils ($r = 0.65$, $p = 0.0003$) and angiosperm and juniper species ACL (*A. rubrum* $r = 0.54$, $p = 0.0002$, *P. occidentalis* $r = 0.75$, $p = 0.0321$, *J. virginiana* $r = 0.52$, $p = 0.0027$) show stronger correlations to mean annual temperature (MAT) than any other environmental parameter (Table 2 and Fig. 5). *P. strobus* ACL is not significantly correlated to MAT and *P. taeda* ($r = -0.55$, $p = 0.0436$) maintains an inverse and weak correlation to MAT. As *P. occidentalis*, *P. strobes*, and *P. taeda* were not sampled as frequently across the environmental gradient and yield no significant relationships to the parameters tested here, and are excluded from further analysis. We focus the remaining statistical analyses and discussion on ACL indices from *n*-alkanes extracted from soils, *A. rubrum* and *J. virginiana*.

PCA indicates that three components explain 99% of the variance with the dataset, with the first component explaining 77% of the variance alone (Table S3). We found MAT, VPD, δD_{MAP} and relative humidity are significantly loaded on the first component, a result of the north–south climate trend of the transect itself (Fig. S3). Precipitation is loaded nearly equally on the first and second component (Table 1).

Temperature accounts for 42%, 27% and 29% of the variation in soil, *J. virginiana* and *A. rubrum* ACL. We find a significant relationship between soil, *J. virginiana* and *A. rubrum* ACL and the first component (PC1), and explains 31%, 24% and 22% of the variation in ACL, respectively (Table 2), suggesting the combination of temperature, humidity and VPD contribute influence leaf wax lipid production.

3.4. δD variation of leaf and soil *n*-alkanes

To compare hydrogen isotope values from the diverse species studied here, we weight individual *n*-alkane δD values according to compound abundance to produce a single mean-weighted *n*-alkane hydrogen isotope ($\delta D_{n\text{-alkane}}$) value for each individual tree (Supplemental Table S2). Hydrogen isotope ratios of species-specific and soil *n*-alkanes span over 112‰ and ranged from $-208‰$ to $-97‰$ (Fig. 6). Our results indicate that $\delta D_{n\text{-alkane}}$ values are most strongly related to latitude and climate variables that co-vary with latitude (Fig. 6). Temperature and δD_{MAP} values are strongly correlated. $\delta D_{n\text{-alkane}}$ values of soil (MAT $r = 0.82$, $p < 0.0001$; δD_{MAP} $r = 0.82$, $p < 0.0001$) and angiosperm *n*-alkanes show the most significant linear correlations to MAT and δD_{MAP} values (*A. rubrum* [MAT $r = 0.94$, $p < 0.0001$; δD_{MAP} $r = 0.92$, $p < 0.0001$], *P. occidentalis* [MAT $r = 0.93$, $p = 0.0003$; δD_{MAP} $r = 0.90$, $p = 0.0010$]). $\delta D_{n\text{-alkane}}$ values of *J. virginiana* *n*-alkanes are weakly correlated to temperature and δD_{MAP} val-
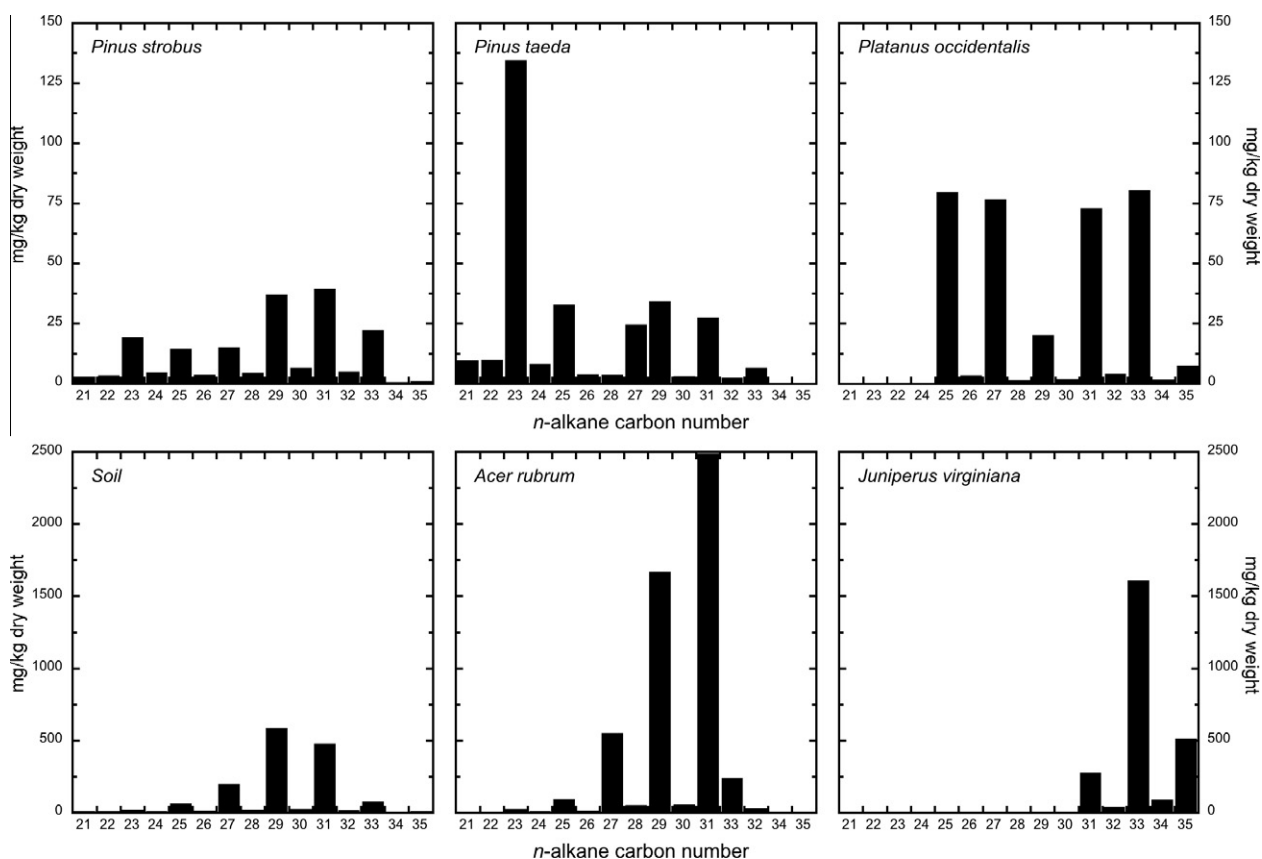

Fig. 4. Histogram of the mean concentration of individual *n*-alkanes from soils and leaf waxes. Concentrations reported as the compound mass relative to the dry leaf mass.
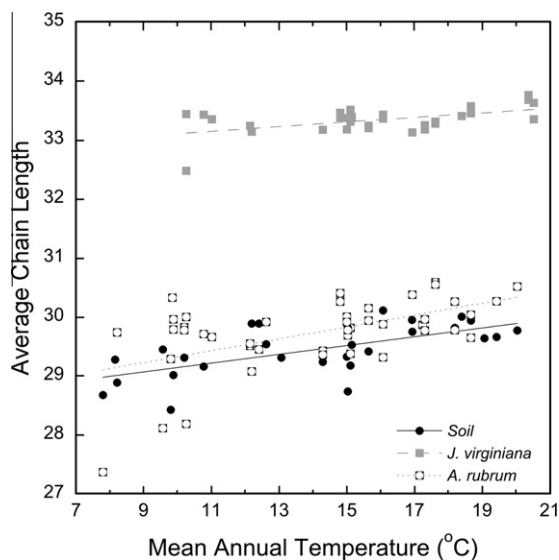
Fig. 5. Cross-plot of average chain lengths from *n*-alkanes extracted from soils, *A. rubrum*, and *J. virginiana* versus mean annual temperature. Average chain length and mean annual temperature correlate with soils ($r = 0.65$, $p = 0.0003$) and individual species ($r = 0.52$, $p = 0.0027$ and 0.54, $p = 0.0002$, respectively).

Table 1
Loading of principal component/factor analysis.

Principal component loadings			
Variable	PC1	PC2	PC3
δD_{MAP}	**0.937**	0.219	0.232
PPT	−0.601	**0.785**	−0.151
MAT	**0.938**	0.226	0.247
RH	**−0.865**	0.046	**0.497**
VPD	**0.984**	0.100	−0.112

Bold and italic denotes values that are statistically significant.

ues (MAT $r = 0.46$, $p = 0.0246$; δD_{MAP} $r = 0.42$, $p = 0.0427$), and *P. strobus* and *P. taeda* are not significantly correlated with either temperature or δD_{MAP} values ($p > 0.05$). *P. occidentalis*, *P. strobes*, and *P. taeda* were not sampled at the same resolution across the environmental gradient, and thus excluded from our evaluation (Fig. 6). Nonetheless, with few exceptions, angiosperms have more positive $\delta D_{n\text{-alkane}}$ values than *Pinus* species from the same site, while $\delta D_{n\text{-alkane}}$ values of *J. virginiana* are greater than angiosperms and pines (Fig. 6).

PCA indicates a significant relationship between $\delta D_{n\text{-alkane}}$ values of soil and *A. rubrum* *n*-alkanes and the first component (PC1), explaining 48% and 79% of the variation, respectively (Table 3). This suggests the combination of δD_{MAP} value, temperature, humidity, and VPD significantly influences both $\delta D_{n\text{-alkane}}$ values of soil and *A. rubrum* *n*-alkanes. PCA indicates a significant relationship between $\delta D_{n\text{-alkane}}$ values of *J. virginiana* *n*-alkanes and the second component (PC2), explaining 19% of the variation (Table 3).

δD_{MAP} values, available for all sites, show a one-to-one correspondence to δD_{XW} values (Fig. 3b). We use δD_{MAP}

values to calculate the apparent isotopic fractionation between *n*-alkanes and source water ($\varepsilon_{n\text{-alkane}}$) defined as:

$$\varepsilon_{n-alkane} = \left(\frac{R_{n-alkane}}{R_{MAP}} - 1 \right) \qquad (8)$$

where $r = D/H$. Average $\varepsilon_{n\text{-alkane}}$ values are $-107 \pm 112‰$ (1σ) for soils, $-113 \pm 8‰$ for the two angiosperm species, $-128 \pm 12‰$ for the two *Pinus* species, and $-89 \pm 12‰$ for *J. virginiana* (Fig. 7). With few exceptions, angiosperm species express more positive $\varepsilon_{n\text{-alkane-MAP}}$ values than *Pinus* species, while *J. virginiana* $\varepsilon_{n\text{-alkane-MAP}}$ values are more positive than the angiosperms and pines from the same site.

Paired *T*-test results between $\varepsilon_{n\text{-alkane}}$ values for soils, angiosperm species, *Pinus* species, and *J. virginiana* indicate that the means for all groups are statistically different ($p < 0.01$) except between $\varepsilon_{n\text{-alkane}}$ values from soils and angiosperm species (Table S4). Further, our results indicate that neither $\varepsilon_{n\text{-alkane}}$ values of angiosperm or gymnosperm species are consistently related to any one variable tested here (Table 3). Soil $\varepsilon_{n\text{-alkane}}$ values are not significantly correlated with any climate variable tested here, while *J. virginiana* $\varepsilon_{n\text{-alkane}}$ values are significantly correlated to all the climate variables and *A. rubrum* $\varepsilon_{n\text{-alkane}}$ values are significantly correlated with all climate variables except precipitation (Table 3).

PCA indicates a relationship between $\varepsilon_{n\text{-alkane}}$ values for *J. virginiana* and *A. rubrum* and the first component (PC1), explaining 37% and 41% of the variation, respectively (Table 3). *J. virginiana* $\varepsilon_{n\text{-alkane}}$ values are negatively correlated to PC1, while *A. rubrum* $\varepsilon_{n\text{-alkane}}$ values are positively correlated to PC1. Soil $\varepsilon_{n\text{-alkane}}$ values are not correlated to any component in this analysis (Table 3).

4. DISCUSSION

4.1. Climatic influence on *n*-alkane distributions

Marked differences in *n*-alkane distributions of the five dominant tree species studied are clearly evident (Fig. 4). Compound distributions among species widely vary, but individual species produce remarkably consistent leaf wax compositions. *J. virginiana* leaf waxes are dominated by *n*-C$_{33}$ and *n*-C$_{35}$. *P. strobes* and *P. taeda* vary in their distribution of *n*-alkanes compared to other species, producing both odd- and even-chain length *n*-alkanes (CPI of 6.8 and 9.8, respectively). Common East Coast conifers produce a wide variety of *n*-alkanes including both the longest (*J. virginiana*) and the shortest (*P. taeda*) chain lengths observed in this study (Fig. 4).

A. rubrum and *J. virginiana* yield longer chain lengths at higher temperatures/lower latitudes (Fig. 5), with MAT explaining 27% and 29% of the ACL variation in *A. rubrum* and *J. virginiana* *n*-alkane distributions, respectively (Table 2) and suggest temperature is the most important control (Table 2). Soil-extracted *n*-alkanes show similar relationships to MAT as *A. rubrum* and *J. virginiana* ACL across the studied gradient (Fig. 5), suggesting that the overall plant community responds similarly to temperature. Sachse et al. (2006) demonstrated that *n*-alkane chain lengths of *Betula*, *Fagus*, and *Quercus* species decrease from

Table 2
Average chain length variation accounted from climate parameters and principal components/factor analysis.

	Soil ACL		J. virginiana ACL		A. rubrum ACL	
	r	p	r	p	r	p
RH	−0.52	0.0050	−0.39	0.0311	−0.22	0.1589
MAT	0.65	0.0003	0.52	0.0027	0.54	0.0002
PPT	−0.25	0.2158	−0.15	0.4068	−0.28	0.0673
VPD	0.45	0.0193	0.47	0.0079	0.40	0.0066
PC1	0.56	0.0027	0.49	0.0051	0.47	0.0012
PC2	0.05	0.8190	0.13	0.4938	0.02	0.9108
PC3	0.43	0.0255	0.00	0.9957	0.28	0.0684

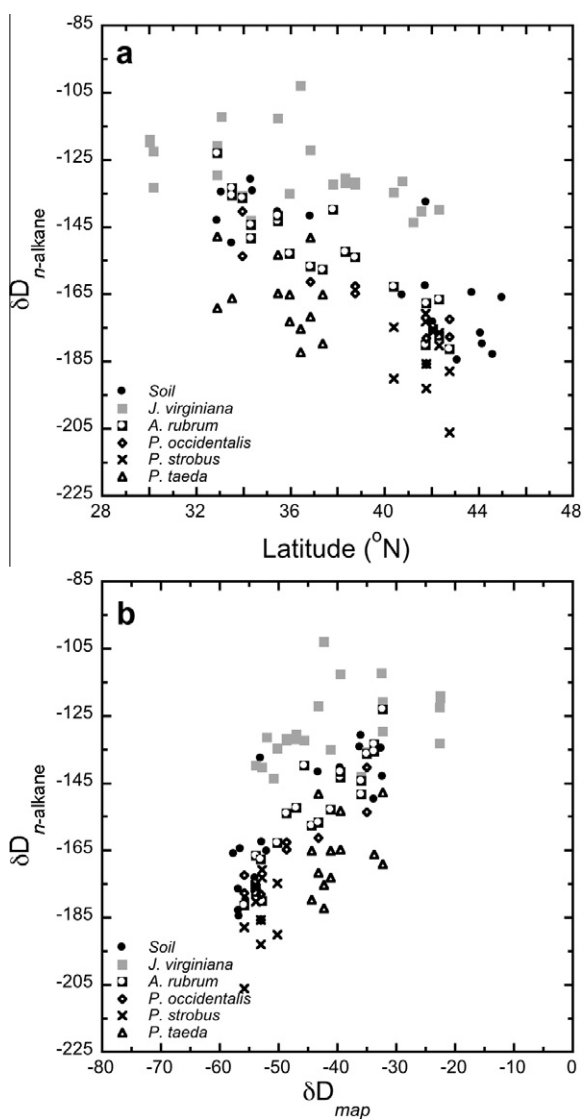Bold and italic denotes values that are statistically significant.

Fig. 6. Hydrogen isotope values of individual species weighted n-alkane versus (a) latitude and (b) hydrogen isotope values of mean annual precipitation.

relationship might be the result of a plant's response to longer growing seasons, increased radiation, in response to water loss or alternatively, evaporative loss of shorter n-alkanes due to increased temperature (Sachse et al., 2006). Similarly, under warmer conditions, plants potentially biosynthesize longer chain-length waxes to limit water loss, given the relationship between a wax carbon length and boiling point (Gagosian and Peltzer, 1986). While the true biosynthetic mechanism is not known, the relative variations in chain-length distributions can be used in paleo-applications when plant community composition or temperature is isolated. n-Alkanes extracted from dust and marine sediments show similar relationships of increased average chain length with decreasing latitude and/or increasing temperature (Schefuss et al., 2003; Hughen et al., 2004). As an example, Smith and colleagues used variations in ACL coupled with macrofossil evidence to model and test $\delta^{13}C$ anomalies during the Paleocene–Eocene Thermal Maximum (Smith et al., 2007). Furthermore, chain length variations have been interpreted during the C_4 expansion during the Late Miocene–Pliocene as plant community change (Tipple and Pagani, 2010).

Soils and soil organic material evolve across hundreds to thousands of years (Van Breeman and Buurman, 2002), and thus represent a spatially and temporally integrated signal of the surrounding ecosystem. Importantly, soil n-alkane ACL values are within the range of the plant n-alkane ACL range, suggesting soil n-alkanes represent a mix of plant n-alkane sources (Fig. 5 and S3). However, even though leaf-litter production is similar for angiosperm and gymnosperm species in temperate forests (Vogt et al., 1986), these chain-length- and concentration data suggest n-alkanes from soils from temperate forests of the Eastern United States are weighted toward angiosperm sources. Recently, large and systematic variations in the concentration of n-alkanes between North American angiosperm and gymnosperm species were reported, with angiosperms producing n-alkane concentrations higher by several orders of magnitude (Diefendorf et al., 2011). Our soil chain-length distributions appear to reflect a similar relationship with angiosperm plants contributing a higher proportion of n-alkanes to soil records. These data suggest that soil-extracted n-alkanes from these types of ecosystems are likely weighted toward angiosperms relative to gymnosperms. Future work should investigate the relative proportions of species in a gi-

higher to lower latitudes. While that work did not focus on the same species for the entire transect, the latitudinal trend appears to be consistent in broad taxonomic groups. This

Table 3
Hydrogen isotope and apparent fractionation variation accounted from climate parameters and principal components/factor analysis.

	Soil $\delta D_{n-\text{alkane}}$		J. virginiana $\delta D_{n-\text{alkane}}$		A. rubrum $\delta D_{n-\text{alkane}}$	
	r	p	r	p	r	p
δD_{MAP}	**0.82**	**<0.0001**	0.42	0.0427	**0.92**	**<0.0001**
RH	−0.30	0.2337	−0.20	0.3491	**−0.74**	**0.0001**
MAT	**0.82**	**<0.0001**	0.46	0.0246	**0.94**	**<0.0001**
PPT	−0.38	0.1153	0.22	0.3044	−0.15	0.5064
VPD	**0.63**	**0.0047**	0.33	0.1101	**0.90**	**<0.0001**
PC1	**0.69**	**0.0015**	0.30	0.1572	**0.89**	**<0.0001**
PC2	0.09	0.7309	0.44	0.0303	0.32	0.1552
PC3	0.37	0.1333	0.04	0.8552	−0.33	0.1410
	Soil $\varepsilon_{n-\text{alkane}}$		J. virginiana $\varepsilon_{n-\text{alkane}}$		A. rubrum $\varepsilon_{n-\text{alkane}}$	
	r	p	r	p	r	p
δD_{MAP}	0.08	0.7379	**−0.57**	**0.0038**	**0.56**	**0.0088**
RH	0.24	0.3392	0.47	0.0191	**−0.59**	**0.0050**
MAT	0.07	0.7858	**−0.57**	**0.0033**	**0.56**	**0.0080**
PPT	−0.14	0.5665	0.45	0.0259	−0.32	0.1584
VPD	−0.11	0.6785	**−0.56**	**0.0047**	**0.63**	**0.0020**
PC1	−0.03	0.9068	**−0.61**	**0.0015**	**0.64**	**0.0019**
PC2	−0.12	0.6432	0.16	0.4640	−0.01	0.9615
PC3	0.39	0.1128	−0.06	0.7966	−0.36	0.1069

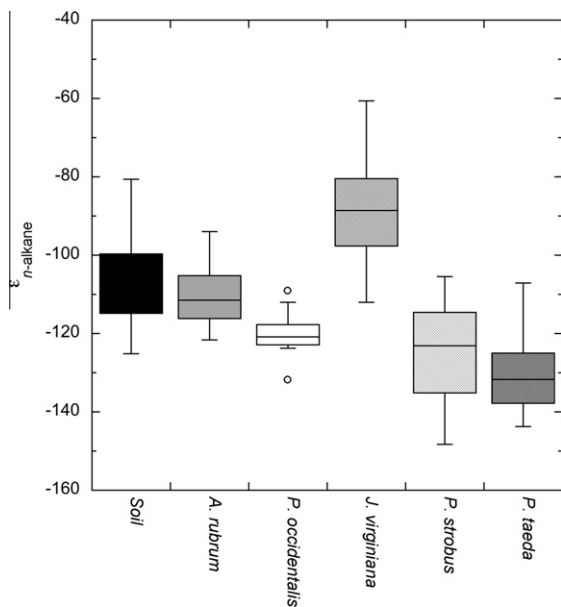Bold and italic denotes values that are statistically significant.

Fig. 7. Individual species and soil n-alkane apparent hydrogen fractionation values. Plot shows median value for each species with the upper (UQ) and lower quartiles (LQ). Outliers are shown with an asterisk and defined as greater than UQ + 1.5 ∗ interquartile distance or less than LQ − 1.5 ∗ interquartile distance.

ven ecosystem and compare n-alkanes in sedimentary records to the ecosystem as a whole.

While significant differences in chain length patterns between species are observed, chain length patterns also correspond to climate. Nonetheless, in sedimentary archives separating plant community change from climate variations based on chain length alone could be problematic without information of ancient plant communities or temperatures.

4.2. Spatial variations in δD_{XW} and $\delta D_{n\text{-alkane}}$ values

The δD value of precipitation along the East Coast of the United States is more D-enriched in the South, and gradually becomes more D-depleted northward. We find a similar pattern in river and stream water (δD_{SW}) along the East Coast transect (Fig. 2a). Groundwater isotope signals are generally similar to long-term average local precipitation isotope composition in these environments (Ofterdinger et al., 2004; Aquilina et al., 2006). However, groundwater isotope ratios can differ significantly from the mean annual isotopic composition of precipitation under specific conditions (Palmer et al., 2007). Our results indicate that δD_{SW} values are most closely related to modeled mean annual δD values of precipitation rather than growing season values (Fig. 3a). While modeled mean annual precipitation cannot specifically identify plant source water, it likely represents the isotopic composition of the long-term average soil moisture available to plants evaluated in this study.

Stem water derives directly from a plant's source water (e.g. soil water, ground water) with no isotopic fractionations (Dawson and Ehleringer, 1993; Dawson et al., 2002). While soil waters were not sampled in this study, stem waters were collected at most locations. We found a one-to-one relationship between δD_{XW} and δD_{MAP} (Fig. 3b), suggesting δD_{MAP} reflect the source water δD value available to the tree in these environments. We restrict our evaluation to δD_{MAP} value because mean annual precipitation data was available at all sites.

$\delta D_{n\text{-alkane}}$ values show a general trend toward more negative values from South to North (Fig. 6a), similar to δD_{XW}, δD_{SW}, and δD_{MAP}, and demonstrate that the D/H ratio of precipitation is the primary control on n-alkane D/H composition (Fig. 6b). However, δD_{XW}, δD_{SW}, and δD_{MAP} values from South to North vary between 40‰ and 50‰, whereas the overall magnitude of change observed in $\delta D_{n\text{-alkane}}$ values is ~110‰ (Fig. 6b). Previous work has also shown large variations in $\delta D_{n\text{-alkane}}$ values between deciduous tree species across environmental transects (Sachse et al., 2006), but not between the same angiosperm and gymnosperm species across an environmental transect. As an example, A. rubrum and J. virginiana were sampled at most sites, but A. rubrum shows a ~60‰ variation with strong relationships to latitude-controlled climate variables, while J. virginiana shows a ~50‰ variation with no significant relationship to any climate variable tested here (Table 3). Several studies have linked variation in $\delta D_{n\text{-alkane}}$ values to life form (Chikaraishi and Naraoka, 2003; Liu et al., 2006; Hou et al., 2007b; McInerney et al., 2011). However, as all individual sampled here were C_3 tree species, life form differences should not apply. There are several potential explanations for observed differences between the angiosperm, A. rubrum and the gymnosperm, J. virginiana.

Epicuticular leaf waxes form during the brief period of leaf expansion in the beginning of the growing season (Kolattukudy, 1970; Riederer and Markstadter, 1996; Jetter and Schaeffer, 2001; Jetter et al., 2006) and their initial leaf wax δD values record a finite period of time (Kahmen et al., 2011). Nonetheless, damage to epicuticular waxes can be repaired or reworked throughout the life of a leave in many species in natural environments (Jetter and Schaeffer, 2001; Nienhuis et al., 2001). J. virginiana keep their leaves for multiple years and the lack of correlation between J. virginiana $\delta D_{n\text{-alkane}}$ values with latitude may be a consequence of a multi-year integration of wax formation and temporal integration. Still, wax synthesis should occur during the same time each season, experience similar temperatures during formation, and record similar $\delta D_{n\text{-alkane}}$ values each year. Alternatively, A. rubrum could be subject to greater leaf-surface abrasion and wax repair during the warmest interval of the growing season relative to J. virginiana. However, this mechanism is unlikely since these two species were collected from the same environments and localities.

J. virginiana living within mixed hardwood forests have been shown to photosynthesize predominately in the early spring, late fall, and even on warm winter days (Lassoie et al., 1983), due to the heavy canopy cover that develops from the broad-leafed angiosperms during the summer. It is possible that J. virginiana biosynthesize leaf waxes during seasons other than the early growing season using different water sources, under different environmental conditions. Furthermore, different climate zones have unique growth seasons and J. virginiana living within these different zones likely photosynthesize at distinct times during the year. Further support for differences in the timing of wax synthesis is shown by these species' δD_{XW} values correspondence with δD_{MAP} values. A. rubrum δD_{XW} and $\delta D_{n\text{-alkane}}$ values correspond to δD_{MAP}, while J. virginiana δD_{XW} values cor-

respond to δD_{MAP}, but not $\delta D_{n\text{-alkane}}$ values. Together, these results suggest that secondary processes (such as evapotranspiration, soil evaporations or timing of wax synthesis) modify individual species leaf waters and complicate the resulting δD signal recorded in individual species leaf waxes.

Soil-extracted n-alkane δD records show a 50–60‰ variation along the transect, similar to water δD values. Similar environmental transect studies using lacustrine sediments demonstrate strong correlations between sediment-extracted n-alkane and precipitation δD values (Huang et al., 2004; Sachse et al., 2004; Hou et al., 2008). This suggests that while secondary processes complicate $\delta D_{n\text{-alkane}}$ values of individual species on a seasonal timescale, soil $\delta D_{n\text{-alkane}}$ records preserve a more integrated, time-average signal – most similar to precipitation δD values.

4.3. Climate controls on n-alkane apparent hydrogen isotope fractionation

The apparent hydrogen isotope fractionation between $\delta D_{n\text{-alkanes}}$ and source water δD values is controlled by soil evaporation, evapotranspiration, and biosynthesis (Sachse et al., 2006). Since evaporation from soils and leaves lead to D-enrichment, $\varepsilon_{n\text{-alkane}}$ values should reflect local evaporative conditions.

In this survey, apparent hydrogen isotope fractionations between $\delta D_{n\text{-alkanes}}$ and δD_{MAP} range from −61‰ to −148‰ with an average fractionation of −108 ± 19‰ (1σ) for all species. While large $\varepsilon_{n\text{-alkane}}$ differences are observed between the different species, we find individual species have relatively stable $\varepsilon_{n\text{-alkane}}$ values (Fig. 7). These values are similar to fractionations reported from other plant and sedimentary studies using tree leaf wax lipids (Chikaraishi and Naraoka, 2003; Huang et al., 2004; Sachse et al., 2004; Hou et al., 2008; Liu and Yang, 2008; Pedentchouk et al., 2008; Zhang and Liu, 2011). While we observe inter-species differences across the transect (Fig. 7), we also discern significant relationships between mean annual temperature, vapor pressure deficit, and δD_{MAP} and J. virginiana and A. rubrum $\varepsilon_{n\text{-alkane}}$ (Table 3). Relationships between these environmental parameters and $\varepsilon_{n\text{-alkane}}$ values have been observed in other natural studies (Smith and Freeman, 2006; McInerney et al., 2011). However in all cases, J. virginiana and A. rubrum $\varepsilon_{n\text{-alkane}}$ values show significant correlations to these climate variables in opposing directions (Table 3). Similarly, PCA indicates a significant relationship between J. virginiana and A. rubrum $\varepsilon_{n\text{-alkane}}$ and PC 1 but with opposing slopes (Table 3).

There are several possible explanations for the observed differences between the A. rubrum and J. virginiana $\varepsilon_{n\text{-alkane}}$ values. Rooting depth differences between these species potentially influence the character of soil water D-enrichment. For example, Feakins and Sessions (2010) show that chaparral plants with deeper rooting depths in very arid environments (southern California) have relatively constant $\varepsilon_{n\text{-alkane}}$ values, but express large differences compared to humid localities, and suggest that moisture availability is a likely reason (Feakins and Sessions, 2010). Direct com-

parisons between *A. rubrum* and *J. virginiana* rooting depth is difficult as *A. rubrum* are more shallowly rooted within the upper 25 cm of the soil, while *J. virginiana* are more adaptable in their rooting habit, with fine fibrous roots on shallow, rocky soils or a deep tap root if soil conditions permit. Thus, *J. virginiana* could be sampling deeper ground waters that are less subject to soil evaporation in some cases, however, the strong correspondence between both species' δD_{XW} and δD_{MAP} values, indicate that at the time of sampling, both species were sampling similar water sources at any given location. However, if *A. rubrum* and *J. virginiana* biosynthesize leaf wax compounds at different times of the year, then it we would not expect consistent results between environment conditions and $\varepsilon_{n\text{-alkane}}$ values across species. These data further suggests that these $\varepsilon_{n\text{-alkane}}$ values from individual species likely reflect differences in the timing of *n*-alkane synthesis.

Soil $\varepsilon_{n\text{-alkane}}$ values are statistically indistinguishable from that of angiosperm $\varepsilon_{n\text{-alkane}}$ values (Table S4) measured along the East Coast transect. Absolute values of soil $\varepsilon_{n\text{-alkane}}$ are consistent with soil $\varepsilon_{n\text{-alkane}}$ values across an elevation transect that covered a similar isotopic range ($\sim$40‰) as our study (Zhang and Liu, 2011). However, in contrast to the individual plants used in that study, we find no relationship between soil $\varepsilon_{n\text{-alkane}}$ and any climate parameters tested here (Table 3). In sum, our results suggest that in specific environments plant species have a wide range of $\varepsilon_{n\text{-alkane}}$ values, but at the ecosystem level, soil $\varepsilon_{n\text{-alkane}}$ values are practically constant across large isotopic and climate gradients. Together, these data suggest that $\delta D_{n\text{-alkane}}$ and $\varepsilon_{n\text{-alkane}}$ from sedimentary archives can be used as a proxy for past precipitation D/H, particularly when independent information of climate and plant community is known.

5. CONCLUSION

In this study, stems and leaves of five co-occurring tree species, including angiosperm species *A. rubrum* and *P. occidentalis* and gymnosperm species *J. virginiana*, *P. taeda*, and *P. strobus*, were sampled along North–South transect along the East Coast of North America. To determine local climate parameters, we used highly resolved temperature, precipitation, and relative humidity data coupled with geographical information software.

We found each species produced a unique distribution of *n*-alkanes with distinct chain length patterns. In addition, we found significant correlations between *A. rubrum*, *J. virginiana* and soil-extracted *n*-alkane average chain lengths and mean annual temperature, suggesting temperature at the time of wax synthesis plays an important role in leaf wax distributions. While statistically significant relationships between *n*-alkane chain length and climate were observed, detecting and interpreting these differences in paleorecords require independent knowledge of temperature or plant community.

Stem water δD values are nearly identical to modeled mean annual precipitation δD values, and suggest mean annual precipitation δD values are equivalent to ground waters in mixed hardwood East Coast forests. Furthermore,

these data suggest that the δD values of stem water can be used along isotope gradients in place of modeled precipitation data when resolution is lacking. When compared to climate data, we found the $\delta D_{n\text{-alkane}}$ value of *A. rubrum* *n*-alkanes strongly correlate to δD values of modeled mean annual precipitation and other climate parameters related to latitude, while the $\delta D_{n\text{-alkane}}$ value of *J. virginiana* *n*-alkanes are not significantly related to modeled mean annual precipitation and any other climate parameter considered in this study. Also, the apparent hydrogen isotopic fractionation between *n*-alkane and mean annual precipitation for both *A. rubrum* and *J. virginiana* correlate to several climate parameters tested. However, in all cases the correlations had opposing relationships. Together, we interpret these findings as evidence that *A. rubrum* and *J. virginiana* produce leaf waxes at different times during the growing season.

We found that soil $\delta D_{n\text{-alkane}}$ values strongly correlate to δD values of modeled mean annual precipitation and other climate parameters related to latitude, while $\varepsilon_{n\text{-alkane}}$ values did not correlate to any climate parameter. These findings indicate that sedimentary $\delta D_{n\text{-alkane}}$ records likely represent an average ecosystem value of mean annual precipitation and can be used as a proxy for the δD values past precipitation, particularly when conditions are similar to Eastern forests of the United States.

APPENDIX A. SUPPLEMENTARY DATA

Supplementary data associated with this article can be found, in the online version, at http://dx.doi.org/10.1016/j.gca.2012.10.042.

REFERENCES

Aquilina L., Ladouche B. and Dorflinger N. (2006) Water storage and transfer in epikarst of karstic systems during high flow periods. *J. Hydrol.* **327**, 472–485.

Bailey R. G. (2002) *Ecoregion-Based Design for Sustainability*. Springer-Verlag.

Bi X., Sheng G., Liu X., Li C. and Fu J. (2005) Molecular and carbon and hydrogen isotopic composition of n-alkanes in plant leaf waxes. *Org. Geochem.* **36**(10), 1405–1417.

Brassell S. C., Eglinton G., Marlowe I. T., Pflaumann U. and Sarnthein M. (1986) Molecular statigraphy: a new tool for climatic assessment. *Nature* **320**(6058), 129–133.

Buck A. L. (1981) New equations for computing vapor pressure and enhancement factor. *J. Appl. Meteorol.* **20**, 1527–1532.

Chikaraishi Y. and Naraoka H. (2003) Compound-specific δD–$\delta^{13}C$ analyses of n-alkanes extracted from terrestrial and aquatic plants. *Phytochemistry* **63**, 361–371.

Coplen T. B. (2011) Guidelines and recommended terms for expression of stable isotope-ratio and gas-ratio measurement results. *Rapid Commun. Mass Spectrom.* **25**, 2538–2560.

Craig H. and Gordon L. I. (1965) Stable isotopes in oceanographic studies and paleotemperatures. In *Deuterium and Oxygen 18 Variations in the Ocean and the Marine Atmosphere*. Consiglio Nazionale Dell Ricerche, pp. 9–130.

Dansgaard W. (1964) Stable isotopes in precipitation. *Tellus* **16**(4), 436–468.

Dawson T. E. and Ehleringer J. R. (1993) Isotopic enrichment of water in the "woody" tissue of plants: implications for plant water source, water uptake, and other studies which use the stable isotopic composition of cellulose. *Geochim. Cosmochim. Acta* **57**, 3487–3492.

Dawson T. E., Mambelli S., Plamboeck A. H., Templer P. H. and Tu K. P. (2002) Stable isotopes in plant ecology. *Annu. Rev. Ecol. Syst.* **33**(1), 507–559.

Diefendorf A. F., Freeman K. H., Wing S. L. and Graham H. V. (2011) Production of *n*-alkyl lipids in living plants and implications for the geologic past. *Geochim. Cosmochim. Acta* **75**(23), 7472–7485.

Eglinton G. and Hamilton R. J. (1967) Leaf epicuticular waxes. *Science* **156**(3780), 1322–1335.

Eglinton T. I. and Eglinton G. (2008) Molecular proxies for paleoclimatology. *Earth Planet. Sci. Lett.* **275**, 1–16.

Feakins S. J. and Sessions A. L. (2010) Controls on the D/H ratios of plant leaf waxes from an arid ecosystem. *Geochim. Cosmochim. Acta* **74**(7), 2128–2141.

Gagosian R. B. and Peltzer E. T. (1986) The importance of atmospheric input of terrestrial organic material to deep sea sediments. *Org. Geochem.* **10**(4–6), 661–669.

Gat J. R. (1996) Oxygen and hydrogen isotopes in the hydrologic cycle. *Annu. Rev. Earth Planet. Sci.* **24**(1), 225–262.

Hou J., D'Andrea W. J. and Huang Y. (2008) Can sedimentary leaf waxes record D/H ratios of continental precipitation? Field, model, and experimental assessments. *Geochim. Cosmochim. Acta* **72**, 3503–3517.

Hou J., D'Andrea W. J., MacDonald D. and Huang Y. (2007a) Evidence for water use efficiency as an important factor in determining the δD values of tree leaf waxes. *Org. Geochem.* **38**(8), 1251–1255.

Hou J., D'Andrea W. J., MacDonald D. and Huang Y. (2007b) Hydrogen isotopic variability in leaf waxes among terrestrial and aquatic plants around Blood Pond, Massachusetts (USA). *Org. Geochem.* **38**(6), 977–984.

Huang Y., Shuman B., Wang Y. and Webb, III, T. (2004) Hydrogen isotope ratios of individual lipids in lake sediments as novel tracers of climatic and environmental change: a surface sediment test. *J. Paleolimnol.* **31**, 363–375.

Hughen K. A., Eglinton T. I., Xu L. and Makou M. (2004) Abrupt tropical vegetation response to rapid climate changes. *Science* **304**, 1955–1959.

Jetter R., Kunst L. and Samuels A. L. (2006) Composition of plant cuticular waxes. In *Biology of the Plant Cuticle* (eds. M. Rieder and C. Muller). Blackwell Publishing, pp. 145–181.

Jetter R. and Schaeffer S. (2001) Chemical composition of the *Prunus laurocerasus* leaf surface. Dynamic changes of the epicuticular wax film during leaf development. *Plant Physiol.* **126**, 1725–1737.

Jia G. D., Wei K., Chen F. and Peng P. A. (2008) Soil *n*-alkane δD vs. altitude gradients along Mount Gongga, China. *Geochim. Cosmochim. Acta* **72**(21), 5165–5174.

Kahmen A., Dawson T. E., Vieth A. and Sachse D. (2011) Leaf wax *n*-alkane δD values are determined early in the ontogeny of *Populus trichocarpa* leaves when grown under controlled environmental conditions. *Plant Cell Environ.* **34**(10), 1639–1651.

Kendall C. and Coplen T. B. (2001) Distribution of oxygen-18 and deuterium in river waters across the United States. *Hydrol. Process.* **15**, 1363–1393.

Kolattukudy P. E. (1970) Cutin biosynthesis in *Vicia faba* leaves. *Plant Physiol.* **46**, 759–760.

Lassoie J. P., Dougherty P. M., Reich P. B., Hinckley T. M., Metcalf C. M. and Dina S. J. (1983) Ecophysiological investigations of understory eastern redcedar in Central Missouri. *Ecology* **64**, 1355–1366.

Liu W. and Yang H. (2008) Multiple controls for the variability of hydrogen isotope compositions in higher plant *n*-alkanes from modern ecosystems. *Global Change Biol.* **14**(9), 2166–2177.

Liu W., Yang H. and Li L. (2006) Hydrogen isotopic composition of *n*-alkanes from terrestrial plants correlate with their ecological life form. *Oecologia* **150**(2), 330–338.

Lockheart M. J., Van Bergen P. F. and Evershed R. P. (1997) Variation in the stable carbon isotope composition of individual lipids from the leaves of modern angiosperms: implications for the study of higher land plant-derived sedimentary organic matter. *Org. Geochem.* **26**, 137–153.

Marzi R., Torkelson B. E. and Olson R. K. (1993) A revised carbon preference index. *Org. Geochem.* **20**, 1303–1306.

McInerney F. A., Helliker B. R. and Freeman K. H. (2011) Hydrogen isotope ratios of leaf wax *n*-alkanes in grasses are insensitive to transpiration. *Geochim. Cosmochim. Acta* **75**, 541–554.

McNab W. H. and Avers P. E. (1994) Ecological subregions of the United States, Vol. 1 (ed. U. S. D. Agriculture). USDA Forest Service.

Nienhuis C., Koch K. and Barthlott W. (2001) Movement and regeneration of epicutiular waxes through plant cuticles. *Planta* **213**, 427–434.

Norman G. R. and Streiner D. L. (2000) *Biostatistics: The Bare Essentials*. B.C. Decker, Inc..

Ofterdinger U. S., Balderer W., Loew S. and Renard P. (2004) Environmental isotopes as indicators for ground water recharge in fractured granite. *Ground Water* **42**, 868–879.

Palmer P. C., Gannett M. W. and Hinkle S. R. (2007) Isotopic characterization of three groundwater recharge sources and inferences for selected aquifers in the upper Klamath Basin of Oregon and California, USA. *J. Hydrol.* **336**(1), 17–29.

Pedentchouk N., Freeman K. H. and Harris N. B. (2006) Different response of δD values of *n*-alkanes, isoprenoids, and kerogen during thermal maturation. *Geochim. Cosmochim. Acta* **70**, 2063–2072.

Pedentchouk N., Sumner W., Tipple B. J. and Pagani M. (2008) Delta C-13 and delta D compositions of n-alkanes from modern angiosperms and conifers: an experimental set up in central Washington State, USA. *Org. Geochem.* **39**(8), 1066–1071.

Peters K. E., Walters C. C. and Moldowan J. M. (2005) *The Biomarker Guide: Biomarkers and Isotopes in the Environment and Human History*. Cambridge University Press.

Piasentier E., Bovolenta S. and Malossini F. (2000) The *n*-alkane concentrations in buds and leaves of browsed broadleaf trees. *J. Agric. Sci.* **135**(3), 311–320.

Poynter J. G., Farrimond P., Brassell S. C. and Eglinton G. (1989) Aeolian-derived higher-plant lipids in the marine sedimentary record: links with paleoclimate. In *Palaeoclimatology and Palaeometeorology: Modern and Past Patterns of Global Atmospheric Transport* (eds. M. Leinen and M. Sarnthein). Kluwer, pp. 435–462.

Riederer M. and Markstadter C. (1996) Cuticular waxes: a critical assessment of current knowledge. In *Plant Cuticles: An*

(ed. G. Kersteins). BIOS Scientific Publishers, pp. 189–200.

Rommerskirchen F., Plader A., Eglinton G., Chikaraishi Y. and Rullkotter J. (2006) Chemotaxonomic significance of distribution and stable carbon isotopic composition of long-chain alkanes and alkan-1-ols in C_4 grass waxes. *Org. Geochem.* **37**, 1303–1332.

Rozanski K., Araguas-Araguas L. and Gonfiantini R. (1993) Isotopic patterns in modern precipitation. In *Climate Change in Continental Isotope Records*, vol. 78 (eds. P. K. Swart, K. C. Lohmann, J. McKenzie and S. Savin). American Geophysical Union, pp. 1–36.

Sachse D., Billault I., Bowen G. J., Chikaraishi Y., Dawson T. E., Feakins S. J., Freeman K. H., Magill C. R., McInerney F. A., van der Meer M. T. J., Polissar P. J., Robins R. J., Sachs J. P., Schmidt H.-L., Sessions A. L., White J. W. C., West J. B. and Kahmen A. (2012) Molecular paleohydrology: interpreting the hydrogen-isotopic composition of lipid biomarkers from photosynthesizing organisms. *Annu. Rev. Earth Planet. Sci.* **40**(1), 221–249.

Sachse D., Kahmen A. and Gleixner G. (2009) Significant seasonal variation in the hydrogen isotopic composition of leaf-wax lipids for two deciduous tree ecosystems (*Fagus sylvatica* and *Acer pseudoplatanus*). *Org. Geochem.* **40**, 732–742.

Sachse D., Radke J. and Gleixner G. (2004) Hydrogen isotope ratios of recent lacustrine sedimentary *n*-alkane record modern climate variability. *Geochim. Cosmochim. Acta* **63**, 4877–4889.

Sachse D., Radke J. and Gleixner G. (2006) δD values of individual *n*-alkanes from terrestrial plants along a climatic gradient – implications for the sedimentary biomarker record. *Org. Geochem.* **37**(4), 469–483.

Sauer P. E., Eglinton T. I., Hayes J. M., Schimmelmann A. and Sessions A. L. (2001) Compound-specific D/H ratios of lipid biomarkers from sediments as a proxy for environmental and climatic conditions. *Geochim. Cosmochim. Acta* **65**, 213–222.

Schefuss E., Ratmeyer V., Stuut J. B. W., Jansen J. H. F. and Sinninghe Damste J. S. (2003) Carbon isotope analyses of *n*-alkanes in dust from the lower atmosphere over the central eastern Atlantic. *Geochim. Cosmochim. Acta* **67**, 1757–1767.

Schimmelmann A., Lewan M. D. and Wintsch R. P. (1999) D/H isotope ratios of kerogen, bitumen, oil, and water in hydrous pyrolysis of source rocks containing kerogen types I, II, IIS, and III. *Geochim. Cosmochim. Acta* **63**(22), 3751–3766.

Schimmelmann A., Sessions A. L. and Mastalerz M. (2006) Hydrogen isotopic (D/H) composition of organic matter during diagenesis and thermal maturation. *Annu. Rev. Earth Planet. Sci.* **34**(1), 501–533.

Schouten S., Hopmans E. C., Schefuss E. and Sinninghe Damste J. S. (2002) Distributional variations in marine crenarchaeotal membrane lipids: a new tool for reconstructing ancient sea water temperatures? *Earth Planet. Sci. Lett.* **204**, 265–274.

Sessions A. L. (2006) Seasonal changes in D/H fractionation accompanying lipid biosynthesis in *Spartina alterniflora*. *Geochim. Cosmochim. Acta* **70**, 2153–2162.

Simoneit B. R. T., Cardoso J. N. and Robinson N. (1991) An assessment of terrestrial higher molecular weight lipid compounds in aerosol particulate matter over the South Atlantic from about 30–70S. *Chemosphere* **23**(4), 447–465.

Smith F. A. and Freeman K. H. (2006) Influence of physiology and climate on dD of leaf wax n-alkanes from C3 and C4 grasses. *Geochim. Cosmochim. Acta* **70**, 1172–1187.

Smith F. A., Wing S. L. and Freeman K. H. (2007) Magnitude of the carbon isotope excursion at the Paleocene–Eocene thermal maximum: the role of plant community change. *Earth Planet. Sci. Lett.* **262**(1), 50–65.

Tipple B. J. and Pagani M. (2010) A 35 Myr North American leaf-wax compound-specific carbon and hydrogen isotope record: implications for C_4 grasslands and hydrologic cycle dynamics. *Earth Planet. Sci. Lett.* **299**, 250–262.

Van Breeman N. and Buurman P. (2002) *Soil Formation*. Kluwer Academic Publishers.

Vogt K. A., Grier C. C. and Vogt D. J. (1986) Production, turnover, and nutrient dynamics of above- and belowground detritus of world forests. *Adv. Ecol. Res.* **15**, 303–377.

Vogts A., Moossen H., Rommerskirchen F. and Rullkotter J. (2009) Distribution patterns and stable carbon isotopic composition of alkanes and alkan-1-ols from plant waxes of African rain forest and savanna C_3 species. *Org. Geochem.* **40**, 1037–1054.

Wakeham S. G. and Pease T. K. (1992) *Lipid Analysis in Marine Particles and Sediment Samples*. Skidaway Institute of Oceanography.

Weijers J. W. H., Schouten S., van den Donker J. C., Hopmans E. C. and Sinninghe Damste J. S. (2007) Environmental controls on bacterial tetraether membrane lipid distribution in soils. *Geochim. Cosmochim. Acta* **71**(3), 703–713.

West A. G., Patrickson S. J. and Ehleringer J. R. (2006) Water extraction times for plant and soil materials used in stable isotope analysis. *Rapid Commun. Mass Spectrom.* **20**, 1317–1321.

Zhang P. and Liu W. (2011) Effect of plant life form on relationship between δD values of leaf wax *n*-alkanes and altitude along Mount Taibai, China. *Org. Geochem.* **42**(1), 100–107.

Associate editor: Josef P. Werne